Supramolecular network design for dynamic and reconfigurable biomedical materials

Dr. J. Fernández[1], Dr. L. Martínez[1], Dr. R. Sánchez[1], Dr. A. Torres[1]*

[1] Department of Internal Medicine and Clinical Research, University of Seville, Seville, Spain

ABSTRACT

With the goal to push the mechanical properties of reconfigurable supramolecular polymers towards those of thermoset resins, we prepared and investigated a new family of hydrogen-bonded polymer networks that are assembled from isophthalic acid-terminated oligo(bisphenol A-co-epichlorohydrin) and different bipyridines. These materials display high storage moduli of up to 3.9 GPa, can be disassembled upon heating to form melts with a viscosity of as low as 2.1 Pa·s, and fully reassemble upon cooling. We show that the new polymers can readily be reconfigured, re-processed or recycled and that the reversible (dis) assembly makes them useful as hot-melt adhesives that permit debonding on-demand.

INTRODUCTION

Commercial thermosets are widely used in the automotive, construction, aerospace, and other industries, as well as in many consumer products.[1] Epoxy resins, which are typically prepared by the reaction of epoxy-based prepolymers with polyfunctional hardeners, are among the most commonly employed thermosets.[1] A wide range of physical properties can be accessed by simple variation of the two components and/or by introducing fillers in the formulation. This approach is for example used to increase the stiffness and strength, or to improve the thermal and/or chemical resistance.[2] The cross-linked nature of epoxies and other thermosets is the basis for their attractive characteristics, but at the same time it stifles reconfiguration, i.e., reprocessing, efficient recycling, or healing of defects.[3] Most solutions that were proposed or are actually employed to recycle or reprocess thermosets are based on physical, thermal, or chemical degradation schemes, which demand high energy input.[3] Chemical approaches typically involve depolymerization at high temperature in the presence of water/solvent mixtures and alkaline or acidic catalysts.[4] This general strategy has been elegantly adapted by several groups who developed reworkable networks based on dynamic covalent bonds such as ester,[5] carbamate,[6] disulfide[7] and urea bonds,[8] or reversible reactions including Diels-Alder chemistry[9] and olefin metathesis[10] among others.[11] An alternative strategy to create reconfigurable materials is the assembly of supramolecular polymers on the basis of non-covalent interactions.[12] The reversible and often dynamic nature of such binding motifs has been utilized to impart polymers with a wide range of stimuli-responsive characteristics,[13] and the possibility to (temporarily) depolymerize such materials upon exposure to an appropriate stimulus has been exploited to create polymers that can be healed[14] or debonded on demand.[15] In principle, this general design approach also permits the creation of reconfigurable supramolecular materials that mirror the

structure and properties of thermosets, but the mechanical properties typically associated with the latter have yet to be achieved. Indeed, with few exceptions,[16] all supramolecular polymers reported to date are based on low glass transition temperature (T_g) building blocks, which enable phase-segregation driven assembly, but afford materials with low stiffness and strength.[14,17] Some of us recently reported a glass-forming supramolecular material based on a low-molecular weight monomer carrying three ureido-4-pyrimidinone (UPy) groups.[18] When cooled from the melt, the trifunctional monomer assembles into a fully amorphous network with a storage modulus of 3.7 GPa. An in-depth investigation revealed that the properties are related to the highly cross-linked architecture and the large content of the binding motif; unfortunately, this feature, and the large association constant of the UPy motif also led to a high melt viscosity and made processing somewhat intricate.

The melt processability of supramolecular polymers can be enhanced by using binding motifs with a low association constant, but in this case phase segregation phenomena must usually be exploited to enable adequate binding and mechanical coherence at room temperature. The vast majority of such materials exhibit elastomer-like properties, and only a few studies have reported high-T_g supramolecular networks.[19]

Among the weakly binding hydrogen bonding motifs found in the literature, the carboxylic acid-pyridine system is perhaps the most versatile and widely employed for the synthesis of supramolecular polymers. Kato and Frèchet pioneered the use of this pair in the synthesis of side- and main-chain liquid crystalline supramolecular polymers.[20] More recently, Wiegel and coworkers studied the liquid crystalline behavior and thermal properties of dynamic networks formed with oligomeric bisbenzoic acids and polyfunctional pyridines.[21] The effect of supramolecular cross-link density on the isotropization temperature of a set of polyacrylates containing benzoic acid and pyridine side-chain units was reported by Lin and Hendrianto.[22] We have recently reported the synthesis of phase segregated supramoleculecular polymers based on the isophthalic acid-pyridine (IPA-Py) hydrogen bonded motif,[23] which was previously used by Kato et al. for the synthesis of non-linear liquid crystalline hydrogen bonded complexes.[24] We employed low-molecular weight bipyridines to cross-link a IPA-terminated telechelic poly(ethylene-co-butylene), which afforded a series of materials whose elastomeric nature is the result of phase segregation between a hard phase formed by the crystalline IPA-Py motifs and a soft phase comprising the telechelic cores. Given these precedents and the simplicity of this supramolecular motif, we sought to apply it to the synthesis of high T_g supramolecular networks whose design is inspired by epoxy resins and merges several elements, including (i) the concept to create supramolecular glasses through the reversible assembly of multifunctional, low-molecular weight building blocks with a high weight fraction of binding motifs;[18] (ii) the utilization of the IPA-Py motif,[25] which has a much lower association constant than UPy and was assumed to permit adequate assembly at low temperatures on the one hand, and complete disassembly during melt processing; and (iii) the use of a glycidyl end-capped oligo(bisphenol A-co-epichlorohydrin) (**1**, $M_n \sim 377$ g/mol) as a high T_g core, which through its polydisperse structure was thought to prevent crystallization.[26] We demonstrate that such materials can be prepared in a surprisingly simple, readily scalable manner by the reaction of **1**, which is the key ingredient for many commercial epoxy resins, with an isophthalic acid (IPA) motif, and assembly of the resulting building blocks with different bipyridines.

EXPERIMENTAL SECTION

Reagents. Phenyl glycidyl ether (99%, Aldrich), glycidyl end-capped oligo(bisphenol A-co-epichlorohydrin) M_n ~ 377 g/mol (Aldrich), 5-aminoisophthalic acid (94%, Aldrich), 4,4′-dipyridyl (98%, Aldrich), 1,2-bis(4-pyridyl)ethane (99%, Aldrich), 4,4′-trimethylenedipyridine (98%, Aldrich), polystyrene-block-polybutadiene-block-polystyrene (M_n = 100,000 g/mol, styrene 30 wt%, Aldrich), 2-(5-chloro-2H-benzotriazole-2-yl)-6-(1,1-dimethylehtyl)-4-methyl-phenol (Tinuvin 326 supplied by Ciba), hydrochloric acid (37%, Aldrich) and Na2SO4 (anhydrous, Aldrich) were used as received. Synthesis grade tetrahydrofuran (THF), ethanol, isopropanol and tert-butanol were used without further purification.

Model aminolysis reaction. Phenyl glycidyl ether (1.0 g, 6.7 mmol), 5-amino isophthalic acid (3.0 g, 16.6 mol), and tert-butanol (10 mL) were combined in a 50 mL round-bottomed flask equipped with a reflux condenser. The reaction mixture was vigorously stirred and heated under reflux overnight, and subsequently filtered hot through a paper filter. The solvent was removed under reduced pressure and the residue was dissolved in THF and precipitated into a mixture of H_2O (50 mL) and HCl (37%, 7 mL). The precipitate was filtered off, re-dissolved in THF, the solution was dried over Na_2SO_4, and the solvent was removed in a rotary evaporator. The resulting solid was purified by column chromatography using C_{18}-functionalized silica and a solvent gradient from H_2O/MeOH 2:1 to H_2O/MeOH 1:1. Three main products were isolated, including the primary aminolysis product (**2**, white powder) and the two diastereomers of the secondary aminolysis product (**3a**, white powder and **3b**, white powder). No isolated yields are reported as this model reaction was performed with the only purpose of identifying the ^{1}H NMR characteristic signals of the primary and secondary aminolysis products that are observed in mixtures **M1** and **M2**.

Analytical data of **2**: ^{1}H NMR (400.0 MHz, DMSO-d6) δ = 12.89 (2H, s, COOH), 7.70 (1H, t, J = 1.4 Hz, CH_{Ar}), 7.45 (2H, d, J = 1.4 Hz, CH_{Ar}), 7.33 – 7.26 (2H, m, CH_{Ar}), 6.99 – 6.92 (3H, m, CH_{Ar}), 6.26 (1H, s, NH), 5.24 (1H, d, J = 4 Hz, OH), 4.04 – 3.93 (3H, m, CH-OH and CH_2-O-), 3.39 – 3.28 (1H, m, CH_AH_B-NH), 3.24 – 3.14 (1H, m, CH_AH_B-NH). ^{13}C NMR (100.6 MHz, DMSO-d6) δ = 167.18 (2C, COOH), 158.56 (1C, C_{Ar}-O), 149.18 (1C, C_{Ar}-NH, IPA), 131.68 (2C, C_{Ar}-COOH, IPA), 129.39 (2C, CH_{Ar}), 120.49 (1C, CH_{Ar}), 117.28 (1C, CH_{Ar}, IPA), 116.32 (2C, CH_{Ar}, IPA), 114.47 (2C, CH_{Ar}), 70.01 (1C, CH_2-O), 67.40 (1C, CH_2-OH), 46.10 (1C, CH_2-NH). ESI+ m/z: 332.1 [M + H].

Analytical data of **3a**: ^{1}H NMR (400.0 MHz, DMSO-d6) δ = 12.99 (2H, s, COOH), 7.77 (1H, s, CH_{Ar}), 7.69 (2H, s, CH_{Ar}), 7.33 – 7.27 (4H, m, CH_{Ar}), 7.03 – 6.93 (6H, m, CH_{Ar}), 5.30 (2H, s, OH), 4.19 – 4.06 (2H, m, CH-OH), 4.00 – 3.91 (4H, m, CH_2-O-), 3.77 (2H, dd, J = 15.1, 3.8 Hz, CH_AH_B-N), 3.59 (2H, dd, J = 15.1, 7.7 Hz, CH_AH_B-N). ^{13}C NMR (100.6 MHz, DMSO-d6) δ = 167.36 (2C, COOH), 158.50 (2C, C_{Ar}-O), 148.22 (1C, C_{Ar}-N, IPA), 131.90 (2C, C_{Ar}-COOH, IPA), 129.42 (2C, CH_{Ar}), 120.58 (1C, CH_{Ar}), 116.92 (1C, CH_{Ar}, IPA), 116.23 (2C, CH_{Ar}, IPA), 114.51 (2C, CH_{Ar}), 69.86 (2C, CH_2-O), 66.57 (2C, CH_2-OH), 54.63 (2C, CH_2-N). ESI+ m/z: 482.1 [M + H].

Analytical data of **3b**: ^{1}H NMR (400.0 MHz, DMSO-d6) δ = 13.01 (2H, s, COOH), 7.77 (1H, s, CH_{Ar}), 7.68 (2H, s, CH_{Ar}), 7.32 – 7.27 (4H, m, CH_{Ar}), 7.02 – 6.92 (6H, m, CH_{Ar}), 5.46 (2H, d, J = 4.7 Hz, OH), 4.19 – 4.07 (2H, m, CH-OH), 3.99 – 3.91 (4H, m, CH_2-O-), 3.85 (2H, dd, J = 15.2, 4.1 Hz, CH_AH_B-N), 3.49 (2H, dd, J = 15.2, 7.5 Hz, CH_AH_B-N). ^{13}C NMR (100.6 MHz, DMSO-d6) δ = 167.26 (2C, COOH), 158.46 (2C, C_{Ar}-O), 148.10 (1C, C_{Ar}-N, IPA), 131.85 (2C, C_{Ar}-COOH, IPA), 129.36 (2C, CH_{Ar}), 120.55 (1C, CH_{Ar}), 117.00 (1C, CH_{Ar}, IPA), 116.23 (2C,

CH_{Ar}, IPA), 114.50 (2C, CH_{Ar}), 69.81 (2C, CH_2-O), 66.52 (2C, CH_2-OH), 54.84 (2C, CH_2-N). ESI+ m/z: 482.1 [M + H].

Isophthalic-acid-terminated oligo(bisphenol A-co-epichlorohydrin) (M1). Glycidyl end-capped oligo(bisphenol A-co-epichlorohydrin) (12.00 g, M_n ~377 g/mol), 5-amino isophthalic acid (40.00 g, 0.22 mol) and tert-butanol (240 mL) were combined in a 1 L round-bottomed flask equipped with a reflux condenser and the white, turbid reaction mixture was vigorously stirred and heated under reflux overnight. At this point, a portion of tert-butanol (160 mL) was distilled off, before the mixture was stirred under reflux for another 7 h. The reaction mixture was filtered hot through a paper filter to remove part of the excess of 5-amino isophthalic acid using 100 mL ethanol to facilitate the process (tert-butanol partially crystallizes at room temperature in the funnel) and ensure full product recovery. Most of the solvent was removed under reduced pressure and a dark brown viscous oil remained, which was re-dissolved in ethanol (250 mL) and precipitated into a mechanically stirred mixture of H_2O (2500 mL) and HCl (37%, 350 mL). The aqueous phase was decanted and the precipitate was purified again by dissolution in ethanol and precipitation into aqueous HCl using the same procedure. The product was then dissolved in ethanol (200 mL), the solution was dried over Na_2SO_4, filtered and the solvent was removed in a rotary evaporator (note that strong foaming was observed). The solid product was subsequently dried overnight in a vacuum oven at 160°C and ca. 0.08 bar to obtain the IPA-functionalized mixture **M1** as a yellowish powder (15.3 g, 65%). Below is the NMR characterization of compound **4**, which is the major product of **M1** (the minor signals belong to branching points introduced by compound **5** and are the same as those assigned to diastereomers **3a** and **3b**), and the ESI-MS data of **M1** in which branched compound **5** is also observed as a minor product (12 mol% according to ^{1}H NMR integration, see Figure S7).

^{1}H NMR (400.0 MHz, DMSO-d6) δ = ^{1}H NMR (400 MHz, DMSO-d6) δ = 12.90 (s, COOH), 7.70 (t, J = 1.2 Hz, end-group CH_{Ar}), 7.44 (d, J = 1.2 Hz, end-group CH_{Ar}), 7.11 – 7.09 (m, CH_{Ar}), 6.90 – 6.82 (m, CH_{Ar}), 6.26 (s, NH), 4.00 – 3.91 (m, CH-OH and CH_2-O-), 3.32 (dd, J = 13.1, 4.4 Hz, CH_AH_B-NH), 3.16 (dd, J = 13.1, 5.9 Hz, CH_AH_B-NH), 1.59 (s, -CH_3). ^{13}C NMR (100.6 MHz, DMSO-d6) δ = 167.22 (COOH, IPA), 156.34 (C_{Ar}-O), 149.22 (C_{Ar}-NH, IPA), 142.64 (C_{Ar}-C(CH_3)), 131.69 (C_{Ar}-COOH, IPA), 127.37 (CH_{Ar}), 117.30 (CH_{Ar}, IPA), 116.35 (CH_{Ar}, IPA), 113.88 (CH_{Ar}), 70.03 (CH_2-O), 67.44 (CH_2-OH), 46.12 (C(CH_3)), 41.15 (CH_2-NH), 30.75 (CH_3). ESI+ m/z: 703 [**4** + H], 987 [**5** + H].

Isophthalic-acid/ethyloxy-terminated poly(bisphenol A-co-epichlorohydrin) (M2). Glycidyl end-capped oligo(bisphenol A-co-epichlorohydrin) (12 g, Mn ~377 g/mol), 5-amino isophthalic acid (40 g, 0.22 mol), and ethanol (600 mL) were combined in a 1 L round-bottomed flask equipped with a reflux condenser. The reaction mixture was stirred and heated to reflux, but turned into an unstirrable suspension after 5 min. After mechanical agitation with a spatula, the mixture became stirrable again and reflux was resumed overnight. At this point, a portion of ethanol (300 mL) was distilled off, before the mixture was stirred under reflux for another 7 h. The reaction mixture was filtered hot through a paper filter to remove part of the excess of 5-amino isophthalic acid and the solid residue was washed with 100 mL of ethanol to ensure full product recovery. The volume of the mixture was reduced in a rotary evaporator to ca. 250 mL and the remaining product was precipitated into a mechanically stirred mixture of H_2O (2500 mL) and HCl (37%, 350 mL). The aqueous phase was decanted and the precipitate was purified again by dissolution in ethanol and precipitation into aqueous HCl using the same procedure. The product was then dissolved in ethanol (200 mL), the solution was dried over Na_2SO_4, filtered and the solvent was removed in a rotary evaporator (note that strong foaming was

observed). The solid product was subsequently dried overnight in a vacuum oven at 160˚C and ca. 0.08 bar to obtain the IPA-functionalized mixture **M2** as a brownish powder (10.7 g, 63% considering an average molecular weight of 534 g/mol calculated from the IPA/ethyloxy ratio obtained by ^{1}H NMR integration). Below is the NMR characterization of compound **6**, which is the major product of **M2** (the minor signals belong to branching points introduced by compound **8** and are the same as those assigned to diastereomers **3a** and **3b**), and the ESI-MS data of **M2** in which compounds **4**, **7** and **8** (branched) are also observed as minor products.

^{1}H NMR (400 MHz, DMSO-d6) δ = 12.90 (s, COOH), 7.69 (t, J = 1.4 Hz, end-group CH_{Ar}), 7.37 (d, J = 1.4 Hz, end-group CH_{Ar}), 7.11 – 7.09 (m, CH_{Ar}), 6.90 – 6.82 (m, CH_{Ar}), 6.21 (s, NH), 3.99 – 3.91 (m, CH-OH and CH_2-O-), 3.47 (q, J = 7.0 Hz, end-group -CH_2CH_3), 3.32 (dd, J = 13.2, 4.6 Hz, CH_AH_B-NH), 3.16 (dd, J = 13.2, 5.9 Hz, CH_AH_B-NH), 1.59 (s, -CH_3), 1.12 (t, J = 7.0 Hz, end-group -CH_2CH_3). ^{13}C NMR (100.6 MHz, DMSO-d6) δ = 167.22 (COOH, IPA), 156.34 (C_{Ar}-O), 149.13 (C_{Ar}-NH, IPA), 142.65 (C_{Ar}-C(CH_3)), 131.71 (C_{Ar}-COOH, IPA), 127.38 (CH_{Ar}), 117.42 (CH_{Ar}, IPA), 116.46 (CH_{Ar}, IPA), 113.89 (CH_{Ar}), 71.63 (CH_2-O-Et), 70.04 (CH_2-O), 69.57 (CH_2-OH), 68.04 (CH_2-O), 67.43 (CH_2-OH), 65.89 (CH_2-CH_3), 46.20 (C(CH_3)), 41.15 (CH_2-NH), 30.74 (CH_3), 15.10 (CH_3). ESI+ m/z: 452.1 [**7** + Na], 590.2 [**6** + Na], 725.1 [**4** + Na]. The branched products (**8**) are only observed by ^{1}H NMR (Figure S9). The integration of the branching points shows that 7 mol% of amino-IPA groups undergo secondary aminolysis to produce branched compound **8**.

Preparation of supramolecular polymers P1a-c and P2a-c. Mixtures **M1** and **M2** were targeted to be mixed with bispyridines **a**, **b** or **c** so the molar ratio between COOH and pyridine groups was 1:1. Due to the polydisperse nature of **M1** and **M2**, it was first necessary to perform a titration of the isophthalic acid end groups, which was achieved by ^{1}H NMR spectroscopy through the following procedure, an example of which is given for **M1**: Three mixtures of **M1** and **a** were prepared (approximately 100 mg **M1**) having theoretical COOH:pyridine ratios of i) 1:1, ii) 1.1:1, and iii) 1:1.1, using a theoretical molecular weight of 739 g/mol (377 g/mol (M_n of glycidyl end-capped oligo(bisphenol A-co-epichlorohydrin)) + 362 g/mol (two amino-IPA residues)) for **M1**. The three mixtures were subsequently dissolved in DMSO-d6 and analyzed by ^{1}H NMR spectroscopy. The cumulative integral of the aromatic signals at 7.75 ppm (CH associated with the isophthalic acid motif at the branching points, Hc-branching point Figure S11) and 7.70 ppm (CH associated with the isophthalic acid motif of the single aminolysis product, Hc Figure S11) was set to 1, and the values of the integrals of the aromatic signal at 8.73 ppm (CH associated with the bispyridine, Ha Figure S11) were collected and plotted against the number of moles of bispyridine in the mixture. A linear fit of the three data points provided the following function: $Integral_{Xppm} = a \cdot moles_{bispyridine} + b$. The exact number of moles of bispyridine required to have a 1:1 COOH:pyridine ratio were then obtained by introducing the value of 4 as the $Integral_{Xppm}$. The integrated ^{1}H NMR spectrum of a sample of **P1a** (**M1** + **a**) prepared on the basis of the result of the above titration procedure is shown in Figure S11. The same titration procedure was used for the mixtures of **M2** with bispyridines **a**, **b** and **c** considering a theoretical molecular weight of 534 g/mol (a value that takes into account the 18 mol% of ethyloxy end groups found by integration of the 1H NMR spectrum). Once titrated, **M1** and **M2** were mixed with the bispyridines to obtain the supramolecular networks. For example, **M1** (4.00 g, 5.41 mmol considering a theoretical molecular weight of 739 g/mol) and **a** (1.53g, 9.79 mmol) were combined in an open 100 mL glass beaker. The mixtures were heated to 180 °C by placing the beaker on a hot plate and mechanically stirred with the aid of a spatula. After a few seconds, the powdery monomers had formed a brown viscous melt that was stirred for 1 min

to ensure full mixing. Upon cooling to room temperature, all mixtures prepared by this process solidified into hard brown solids that strongly adhered to the beaker. The materials were scraped off with the help of a spatula, ground in a mortar to obtain a fine powder, which was melted again in an open beaker by heating to 180 °C and kept at this temperature for 30 min, before the material was cooled to room temperature and ground once more. The resulting powders (**P4a-c** and **P5a-c**) were used as hot-melt adhesives or were further melt-processed into rectangular samples for 3-point bending tests.

Preparation of samples for 3-point bending, differential scanning calorimetry and infrared spectroscopy analyses. A home-made rectangular mold with the dimensions 3 x 1 x 1 cm, featuring a steel bottom (to permit heat transfer) and sides made from poly(tetrafluoroethylene) was used to prepare the specimens used for the 3-point bending tests. We observed that the materials studied here adhere strongly to different surfaces, including steel and poly(tetrafluoroethylene), and that they shrink considerably upon solidification from the melt, leading to the formation of cracks upon cooling. The bottom and sides of the mold were thus lined with flexible poly(tetrafluoroethylene) tape to limit the effects of contraction upon cooling. Powdered P1a-c or **P2a-c** (1 g) were put in the mold, which in turn was placed for 30 min in an oven heated to 180 °C. After removing the mold from the oven and cooling to ambient temperature, the samples were demolded and all sides were smoothened by polishing with sand paper (grit size P220) to obtain homogeneous, rectangular samples with dimensions of approximately 3.00 x 0.70 x 0.25 cm. The exact dimensions of the samples were measured with a caliper (accuracy = 10 μm) before DMA analysis. The samples thus processed were also used for DSC and FT-IR analyses.

Characterization. ^{1}H-NMR and ^{13}C-NMR spectra were recorded in DMSO-d6 on a Bruker 400 spectrometer operating at 400 MHz and 100.6 Hz respectively. Chemical shifts (δ) are reported in parts per million relative to tetramethylsilane, although referencing was done based on the solvent signal (DMSO, δ = 2.50 ppm). The relaxation time (d1) was set to 5 s. Fourier transform infrared spectroscopy (FT-IR) spectra were acquired on a Perkin Elmer Spectrum 65 spectrometer in attenuated total reflectance (ATR) mode between 4000 - 600 cm^{-1} with a resolution of 4 cm^{-1} and 50 scans per sample. Electrospray ionization mass spectrometry (ESI-MS+) was performed on a Bruker FTMS 4.7T BioAPEX II. Differential scanning calorimetry (DSC) studies were carried out with a Mettler-Toledo STAR system under nitrogen atmosphere using a sample mass of approximately 5 mg. The glass transition temperatures (T_g) reported are the midpoints of the step change in the heat capacity. Thermal degradation studies were performed on a Mettler-Toledo TGA/DSC STARe System at a heating rate of 10 °C/min from 25 °C to 500 °C with samples of 10 mg in 40 μL aluminum crucibles. Small- and Wide-angle X-ray scattering (SAXS, WAXS) spectra were recorded with a NanoMax-IQ camera (Rigaku Innovative Technologies, Auburn Hills, MI USA). The samples were kept in vacuum at room temperature during the measurements. Raw data were processed according to standard procedures, and the scattering spectra (1d) are presented as a function of the momentum transfer $q = 4\pi \cdot \lambda^{-1} \cdot \sin(\theta/2)$, where θ is the scattering angle and λ = 0.1524 nm is the photon wavelength. Dynamic mechanical analyses (DMA) were conducted in a 3-point bending set-up with a TA Instruments DMA Q800 at a heating rate of 3 °C min^{-1}, from 25 °C to 150 °C, at a frequency of 1 Hz and an amplitude of 5 μm, using rectangular samples of the following approximate dimensions: 3 cm x 0.70 cm x 0.25 cm. Storage moduli and the 1 GPa temperature threshold (T_{1G}) are reported as the average of 3 independent tests. Rheological studies were performed on a TA instruments AR-G2 rheometer with a Peltier-element-controlled temperature parallel plate

setup. Temperature dependent shear moduli and viscosity data of **P1a-c** and **P2a-c** were acquired at 20 rad/s at temperatures between 190 °C and 90 °C at temperatures 5 °C apart. Frequency sweep experiments (30 data points between ω = 0.05 and ω = 100 rad/s) were conducted at 200 °C for **M2** and 180 °C for **P1a-c** and **P2a-c**. For clarity we report temperature-dependent data for only one frequency. Adhesion tests were performed at room temperature using a Zwick/Roell Z010 tensile tester equipped with a 10 kN load cell and mechanical gripping clamps with a strain rate of 10 mm/min. Lap joints were made with stainless steel slides with bond areas of 10 × 10.1 mm by applying 10 mg of each powdered material, heating above the glass transition temperature (typically 150 °C) and pressing both slides while cooling the sandwich to ambient temperature. Reported shear strengths are averages of 6 independent measurements. Moisture uptake analyses were performed as reported elsewhere,[27] using closed chambers containing a saturated solution of NaCl or K_2SO_4 to maintain a relative humidity of 75% or 97%, respectively. The samples (ca. 0.7 g) were removed from the chambers at specific time points (i.e. daily), wiped with tissue paper to remove superficial water, and weighed on a four-digit analytical balance. UV-light debonding experiments were performed with a Hönle Bluepoint 4 Ecocure UV lamp equipped with an optical fiber, a 320−390 nm filter and an intensity of 1600 mW/cm^2. The surface temperature of **P2c** and SBS copolymer upon UV irradiation was monitored with an Optris PI Connect infrared camera (model PI 160) from Roth AG (Switzerland).

RESULTS AND DISCUSSION

In order to develop a better understanding of the nature of the products formed, we first conducted a model reaction between phenyl glycidyl ether and 5-aminoisophthalic acid (**aminoIPA**, Scheme 1a). All reactions were carried out without a catalyst, to favor epoxide aminolysis and avoid attack of the epoxides by the carboxylic acids. The reaction was performed in tert-butanol, which for steric reasons does not cause alcoholysis of the epoxy groups. An excess of 2.5 eq. of **aminoIPA** per epoxide was required to achieve full conversion of the epoxy groups. Aminolysis adduct **2** and an equimolar amount of the secondary aminolysis adduct **3** (determined by ^{1}H NMR spectroscopy, see SI) were obtained.

Two sets of conditions were applied for the reaction between **1** and **aminoIPA**. **1** was first reacted with 3.4 eq. (the minimum required to achieve full conversion of the epoxy groups) **aminoIPA** in tert-butanol, to afford a mixture (**M1**) of the difunctional **4** (88 mol%, per ^{1}H NMR analysis, Supporting Figure S8) and the trifunctional **5** (12 mol%), which was formed by secondary aminolysis of **1** with **4** (Scheme 1b). This simple one-pot procedure was conducted without catalyst, the purification by precipitation in acidic water was straightforward, and **M1,** which was isolated in a yield of up to 65%, was free of unreacted epoxides. We also reacted **1** with 3.4 eq**. aminoIPA** in ethanol (Scheme 1b) to produce a mixture (**M2**) of **4**, the ethoxylated, mono- (**6**) and difunctional (**7**) building blocks, and the branched product **8**. Thus, upon assembly into hydrogen bonded networks with difunctional pyridines, **M2** should lead to fewer cross-links, and the free 1,3-ethylphenyl glycerol ether residues should serve as plasticizers. Indeed, the T_g (114 °C) of a sample of **M2** was considerably lower than that of **M1** (132 °C, Figure 2a).

Scheme 1. a) Model reaction of phenyl glycidyl ether and aminoIPA. b) Synthesis of IPA-modified oligo(bisphenol A-co-epichlorohydrin) mixtures **M1** and **M2**. c) Components used to prepare supramolecular networks **P1a-c** and **P2a-c**.

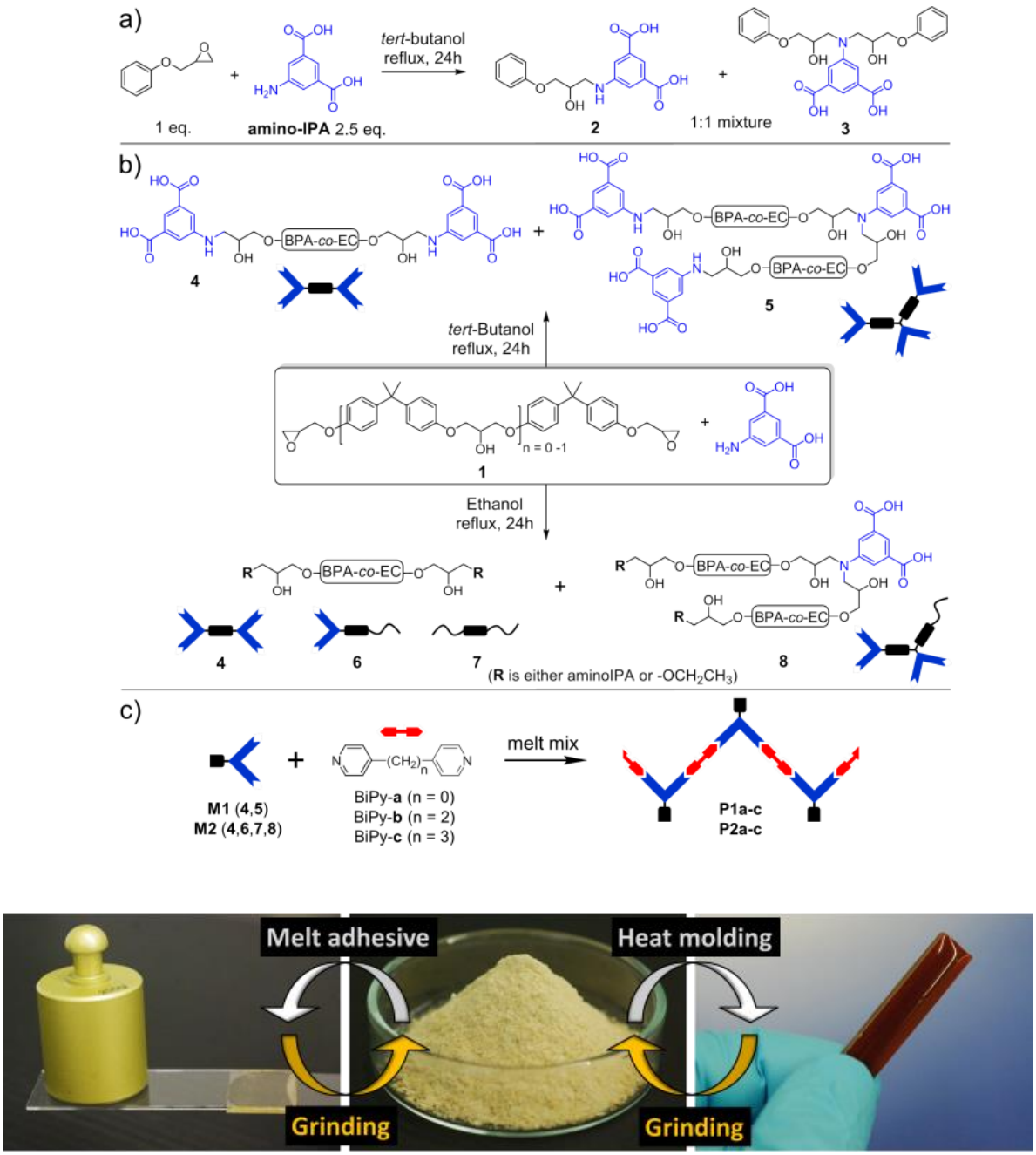

Figure 1. Pictures showing a lap-joint formed by two glass slides and **P2b** (left, the weight is 200 g), **P2b** in powder form (center) and a melt-processed bar of **P2b** (right).

The IPA-modified oligo(bisphenol A-co-epichlorohydrin) mixtures **M1** and **M2** were combined with the three commercial bipyridines **a-c** to prepare two series of supramolecular networks **P1a-c** and **P2a-c** (Scheme 1c). In all cases, the COOH:pyridine ratio was equilibrated according to the results of ^{1}H NMR titrations of **M1** or **M2** with each bipyridine (Supporting Figure S11),[25] and the components were mechanically mixed in the absence of solvent at 150 °C. While the neat **M1** and **M2** do not flow at this temperature, the addition of the bipyridines lead to the formation of viscous melts, which solidified upon cooling into rigid solids that adhere tenaciously to glass or steel. The materials were then subjected to two melting-grinding cycles

(see Experimental Section), to afford yellowish to brownish powders, which were melt-processed and used as adhesives or specimens for mechanical testing (Figure 1). This procedure was found to be essential to ensure good mixing of the components and to obtain materials with reproducible mechanical properties, as will be discussed below. The coloring observed upon melt-processing does not affect the basic structure of the supramolecular networks nor their mechanical properties. Indeed, both **M1** and **M2** are brown solids and the further coloring observed is similar to the well-known thermal yellowing of thermosets such as epoxy resins,[28] which may possibly be suppressed by the use of stabilizers, if desired. A comparison of the FT-IR spectra (Supporting Figure S13) of the neat **M1** and **M2** and the supramolecular networks **P1a-c** and **P2a-c** shows a clear shift of the carbonyl band from 1693 cm^{-1} (H-bonded COOH dimer) to 1698 cm^{-1} (COOH-pyridine bond) in all samples, confirming the formation of COOH-pyridine H-bonded networks.[29]

The differential scanning calorimetry (DSC) thermograms of mixtures **M1** and **M2** and the supramolecular networks **P1a-c** and **P2a-c** (Figure 2) show single glass transitions between 73°C and 132 °C followed by small endothermic events and suggest that these materials are substantially amorphous. Unlike the materials reported by Griffin et al., which crystallized upon heating, neither of the materials investigated here shows cold crystallization and their glass transition temperatures are also substantially higher. While the structure and molecular weight of the building blocks **M1** and **M2** are reminiscent of molecular glasses that form persistently amorphous high T_g phases without forming supramolecular polymers,[30] we will show below that they exhibit features that are consistent with hydrogen-bonded networks formed through acid dimerization. As expected on account of the higher carboxylic acid content and the absence of plasticizing 1,3-ethylphenyl glycerol ether groups, the T_g values of the series made with monomer mixture **M1** are slightly (ca. 10 °C) higher than those assembled from **M2** (Table 1). The only thermal transition seen in the DSC traces of **P1a-c** and **P2a-c** is a T_g that is different from that of **M1** and **M2**, respectively, which is consistent with (although taken alone not conclusive) the formation of supramolecular networks through carboxylic acid-pyridine hydrogen bonding. The T_g values follow the same trend within both series (**P1a-c** and **P2a-c**), decreasing with the number of methylene groups in the bipyridine.

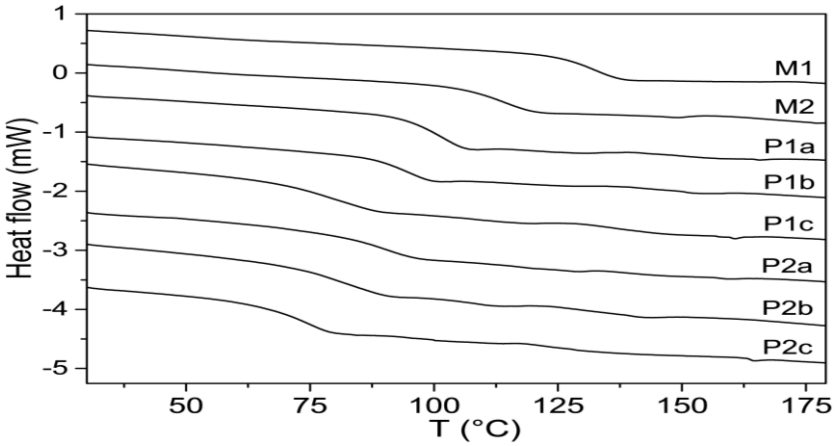

Figure 2. DSC traces (heating rate = 10 °C/min) of IPA-functionalized mixtures **M1** and **M2**, and of the supramolecular networks **P1a-c** and **P2a-c**.

The combined SAXS/WAXS spectra of all supramolecular networks show a feeble and broad correlation peak between q = 1.7 nm^{-1} (d = 3.7 nm) and q = 5.9 nm^{-1} (d = 1.1 nm), and an amorphous halo that is superimposed with a few very small sharp peaks (Figure 3). Unlike all other samples, **P1c** shows some degree of phase separation as evidenced by the broad shoulder centered at ca. q = 0.8 nm^{-1}. We have observed a similar behavior in low-T_g phase segregated supramolecular polymers, where the supramolecular unit formed via hydrogen bonding of IPA and bipyridine **c** led to more efficient phase segregation than in supramolecular polymers with bipyridines **a** or **b**.[25] On the other hand, the lower content of IPA-Py motifs in the less functionalized **P2c** seems to prevent the same phase segregation. The peaks observed at high q values may be due to the crystallization of a very small fraction of IPA-Py motifs, which are common to all materials and would explain the endothermic events observed in the thermograms. Indeed, the peaks at q = 18.2 nm^{-1} (d = 3.4 Å) and q = 22.0 nm^{-1} (d = 2.8 Å) point to π-π stacking[31] and pyridine-carboxylic acid hydrogen bonding.[23] We subsequently studied the evolution of these supramolecular networks at room temperature and analyzed samples that had been kept in a desiccator for 4 months. The DSC traces (Figure S16) showed virtually unchanged thermal properties and the SAXS/WAXS spectra (Figure S15) confirmed the stability of these materials in the studied time/temperature range; with the exception of **P1a** and **P1c**, whose spectra showed some phase segregation, no major changes could be observed.

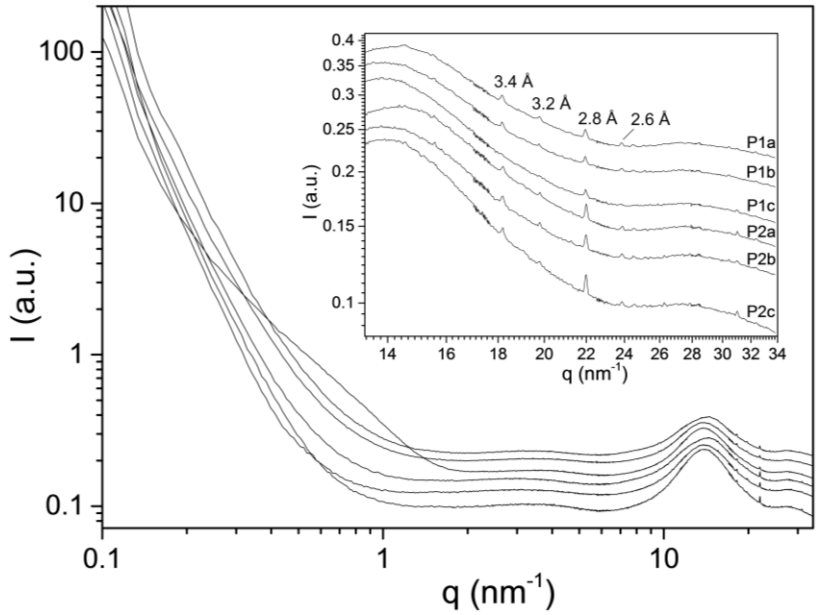

Figure 3. Combined SAXS/WAXS spectra of **P1a-c** and **P2a-c** (the order is the same as in the inset). The inset shows a close up of the high q region. All samples had been heated for 30 min at 180 °C and were then cooled to ambient before measuring.

Table 1. Thermal, mechanical and adhesive data of **P1a-c**, **P2a-c** and of recycled samples **P1b1-2**.

Sample	E′ at 30 °C[a] (GPa)	T_{1GPa}[a] (°C)	T_g[b] (°C)	τ[c] (MPa)
P1a	3.9 ± 0.1	132 ± 1	100	1.4 ± 0.2

P1b	3.9 ± 0.1	124 ± 1	94	1.4 ± 0.2
P1c	3.5 ± 0.1	112 ± 1	81	1.4 ± 0.3
P2a	3.9 ± 0.1	121 ± 1	89	1.5 ± 0.1
P2b	3.8 ± 0.1	115 ± 3	83	1.4 ± 0.1
P2c	3.5 ± 0.1	103 ± 1	73	1.4 ± 0.1
P1b1	3.7 ± 0.2	124 ± 1	-	1.6 ± 0.1
P1b2	3.8 ± 0.1	126 ± 2	-	1.4 ± 0.2

[a]Storage modulus and failure temperature determined by DMA. [b]Glass transition temperature determined by DSC. [c]Shear strength of single lap-joint formed by bonding two stainless steel substrates.

While mixing **M1** with pyridine (using a 1:1 ratio of COOH:pyridine groups) afforded a soft malleable solid with the consistency of modelling clay, the corresponding supramolecular networks **P1a-c** and **P2a-c** are rigid solids. To quantify their mechanical properties, all materials were melt-processed into test bars by heating the as-prepared powders for 30 min at 180 °C in a mold and subsequent cooling to ambient. The resulting samples are brownish, feature glossy surfaces (Figure 1) and were sufficiently tough to be sanded for the preparation of specimens for mechanical analysis. Dynamic mechanical analyses (DMA) in a 3-point bending test configuration (Figure 4a) reveal traces with similar features for all compositions. A largely constant storage modulus E′ is seen below T_g, which gradually decreases above T_g until failure occurs. At room temperature, all materials are highly rigid, with E′ of 3.5 – 3.9 GPa (Table 1). The stiffness is slightly higher for the series based on **M1** and decreases within both series with increasing spacer length of the bipyridine motif. The failure temperature (expressed as the temperature at which E′ has dropped to 1 GPa, T_{1GPa}) follows the same trend as the T_g, with values decreasing linearly from **P1a** to **P1c** and from **P2a** to **P2c**.

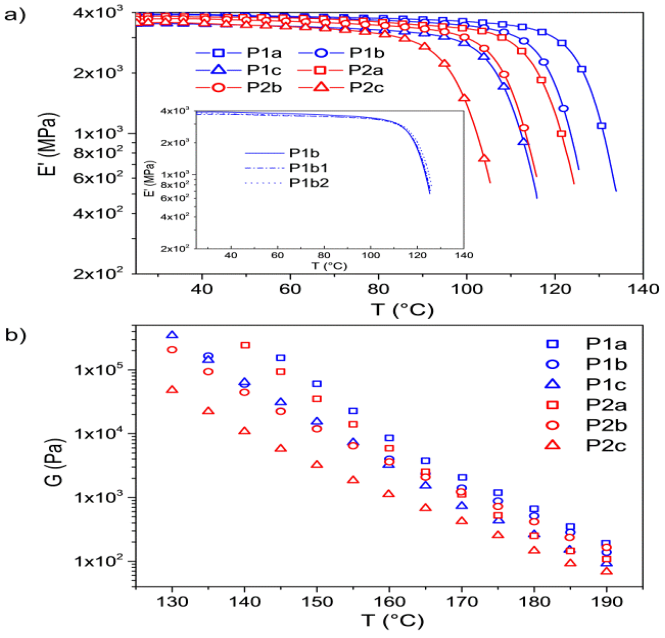

Figure 4. a) Storage moduli E' of **P1a-c** and **P2a-c** as function of temperature, measured by dynamic mechanical analysis (DMA) in a 3-point bending test. The inset shows DMA traces of a pristine sample (**P1b**) and samples that were reprocessed once (**P1b1**) or twice (**P1b2**). b) Shear moduli G of **P1a-c** and **P2a-c** as a function of temperature measured at 20 rad/s.

The rheological behavior of **P1a-c** and **P2a-c** above T_g was probed in a rheometer with a temperature-controlled parallel plate setup. The shear modulus (G, Figure 4b) and viscosity (η, Supporting Figure S17, and Table S1) decrease significantly and in a nonlinear manner upon heating, indicating a gradual shift of the equilibrium from a supramolecular network towards the monomer side, i.e., a decrease of the virtual molecular weight. The trends observed for G and η mirror the solid-state mechanical behavior and the plots converge at high temperature, arguably due to the increasing influence of the monomer melt viscosity. Low melt viscosities (between 2.1 and 6.9 Pa·s, see Supporting Table S1) comparable to those of previously reported supramolecular elastomers[32] were observed for all samples at 190 °C, reflecting that at this temperature these new materials are easy to process and recycle.

Figure 5 shows the frequency dependence of the elastic and viscous moduli as well as the complex viscosity of **M2**, **P1a** and **P1b** at a temperature well above T_g (at least 80 °C higher). The melt properties of **M1** could not be studied as its viscosity was too high below the decomposition temperature, and the frequency sweeps for **P1b-c** and **P2b-c** can be found in the supporting information (Supporting Figure 18). A strong frequency dependence of the mechanical properties was observed for all materials, which show similar G′ and G′′ profiles with three different regimes including a viscous flow at low ω, an intermediate regime in which G′ ~ G′′ for most materials except for **M2**, which showed an elastic plateau, and a dissipative regime at high ω. These data suggest that in the melt the materials are not cross-linked, but behave like lightly entangled polymers.[33]

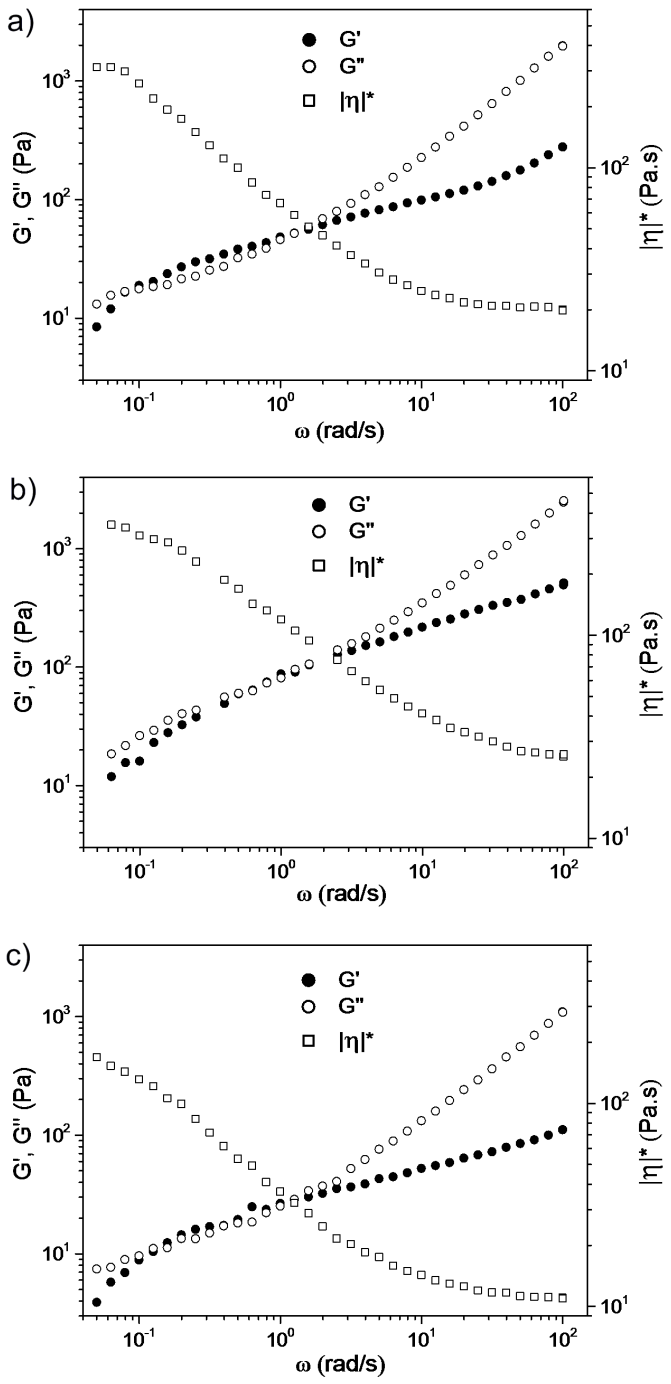

Figure 5. Frequency dependence of the elastic (●) and viscous (○) moduli and the complex viscosity (□) of a) **M2** (at 200 °C), b) **P1a** (at 180 °C) and c) **P2a** (at 180 °C).

To demonstrate the recyclability and reconfigurability in general, samples of **P1b** that had been used in a DMA experiment and mechanically failed upon heating were powderized and remolded using the original processing conditions (**P1b1**). The samples were characterized and recycled again in an analogous manner (**P1b2**). Gratifyingly, the DMA traces of the original and recycled samples (Table 1, Figure 4a, inset) show no significant difference. The reprocessed materials readily dissolved in deuterated DMSO and their ^{1}H NMR spectra confirm the stoichiometric

ratio between carboxylic acid and pyridine groups (Supporting Figure S20). Thus, the formation of the supramolecular network is indeed fully reversible. The thermal stability was further probed by monitoring the melt viscosity of **P1b** at 180 °C over time, applying a constant shear rate (Figure S19). A slight but steady increase of viscosity was observed over time, but even after 4h the material remained soluble in DMSO-d6, ruling out substantial covalent cross-linking. Although ^{1}H-NMR spectroscopy revealed the partial degradation (Figure S20), the reversibility of the networks was not lost.

In order to probe how exposure to moisture affects the new supramolecular polymers, samples of **P1b** were conditioned at a relative humidity (RH) of 75% for 6 days. Interestingly, a weight gain of only 0.72 ± 0.07% was observed (Figure S21), which increased to 1.96 ± 0.11% after the samples had been conditioned for another 7 days at 97% RH. However, premature failure in most of the samples was observed when they were subjected to mechanical testing. Thus, while the exposure of the new materials to moisture results in only a very low water uptake, it causes severe structural damage, arguably by weakening or disruption of the hydrogen bonded network.

We have previously reported the usefulness of much softer supramolecular polymers as adhesives that permit (de)bonding on demand, and demonstrated the possibility to heal defects upon heating or exposure to light.[15,34] Thus, we sought to explore if the supramolecular polymer networks introduced here offer the same functionalities. The adhesive properties of these materials were investigated by testing single lap-joints formed by bonding two stainless steel substrates with **P1a-c** or **P2a-c**. These were made by placing the polymer powders between the steel sheets, heating this sandwich quickly to 150 °C and cooling to ambient under gentle pressure. The shear strength, determined by uniaxial deformation (Table 1, Supporting Figure S22), ranged from 1.4 – 1.5 MPa and showed hardly any dependence on the composition. All samples failed through a mixture of cohesive and adhesive modes, although the latter was a bit more prominent (Figure S23), indicating a relatively strong interaction with the steel surface. On account of the re-configurability of the new supramolecular polymers, samples that had failed during mechanical testing could readily be re-bonded by simply re-positioning the substrates, heating, and cooling. Thus, the shear strength of an original lap joint formed with **P1b** and specimen that had been rebounded once (**P1b1**) or twice (**P1b2**) are virtually indistinguishable. In a qualitative experiment (see supporting movie 1), two glass slides were bonded with **P2a** by placing the powder between the substrates, melting it and applying gentle pressure while cooling to room temperature. After only ca. 10 s, the lap joint thus formed could hold a 500 g weight. The bond could be instantaneously be released upon heating on account of the low melt viscosity of the supramolecular material and rebonding was also possible (the process was repeated up to three times). It was also possible to achieve on-demand debonding by using UV-light as a remote stimulus.[15] On account of the high content of aromatic groups, which act as UV-light/heat converters due to non-radiative decay of the optically excited states,[35] the supramolecular networks **P1a-c** and **P2a-c** can be heated upon exposure to UV radiation (Figure S24). For instance, the temperature of **P2c** increased to ca. 140 °C (Figure S24) after only 5 s of irradiation with a UV-light source (λ = 320-390 nm, I = 1600 mW/cm^2) and to 270 C after 20 s, where the material showed signs of decomposition. When a lap joint formed with 1 mm thick glass substrates and a ca. 300 μm thin layer of **P2c** was irradiated with UV light (λ = 320-390 nm, I = 1600 mW/cm^2), debonding was achieved within 14 s (supporting movie 2). While the debonding time depends on the experimental conditions, this represents an improvement over other supramolecular adhesives developed in our group.[34,36] For comparative purposes, we performed the same debonding experiment with a poly(styrene-b-butadiene-b-styrene) block copolymer (SBS,

M_n = 100,000 g/mol, S content = 30 %), a typical component of hot-melt adhesives. Figure S24 shows that under otherwise identical experimental conditions, the SBS copolymer heats up to only 70 °C after 30 s of irradiation and no debonding was observed even after 2 min of irradiation. To achieve more effective light/heat conversion, we blended the SBS copolymer with 0.25 wt% of Tinuvin 326 (solvent cast from $CHCl_3$), a very efficient UV-light-heat converter.[34,36] As can be seen in Figure S24, the SBS/Tinuvin 326 blend could be rapidly (15 s) heated to ca. 250 °C by UV irradiation, but in sharp contrast to **P2c**, debonding occurred only after 62 s of irradiation. These results illustrate the fundamental difference between the present supramolecular polymers and conventional thermoplastics. While the former display monomer-like melt behavior, the latter are also in the melted state highly viscous, as a result of persistent chain entanglements.

CONCLUSIONS

In summary, the hydrogen bonded, epoxy-resin inspired supramolecular networks presented here display a new combination of properties, which include low melt viscosity, high room temperature moduli, good adhesion to steel and glass surfaces and UV-responsiveness. The proposed synthetically undemanding, scalable two-component approach allows for easy property tuning. Importantly, the new materials can be reconfigured without significant property changes. Thus, the proposed framework provides a basis that may open the way for the development of new supramolecular materials displaying attractive mechanical properties while maintaining high processability and stimuli responsiveness.

ASSOCIATED CONTENT

Supporting Information. NMR, TGA, FT-IR, DSC, SAXS-WAXS, Rheology, moisture uptake analysis, adhesion tests and temperature vs. time profiles under UV irradiation are available free of charge via the Internet at http://pubs.acs.org.

AUTHOR INFORMATION

Corresponding Author

*E-mail: lucas.montero@unifr.ch.

Author Contributions

The manuscript was written through contributions of all authors. All authors have given approval to the final version of the manuscript.

ACKNOWLEDGMENT

We acknowledge financial support from the Adolphe Merkle Foundation and the Swiss National Science Foundation (SNSF). LME is grateful for support through the Ambizione program of the SNSF. DWRB acknowledges funding from the U.S. Army Research Office (W911NF-12-1-0339).

REFERENCES

(1) Chung, D. D. L. In Composite Materials; Springer: London, 2010, p 131-156.

(2) Derek, H.; Clyne, T. W. An introduction to composite materials; Cambridge university press, 1996.

(3) Pickering, S. J. Recycling technologies for thermoset composite materials—current status. Composites, Part A **2006**, 37, 1206-1215.

(4) Oliveux, G.; Dandy, L. O.; Leeke, G. A. Current status of recycling of fibre reinforced polymers: Review of technologies, reuse and resulting properties. Prog. Mater. Sci. **2015**, 72, 61-99.

(5) (a)Montarnal, D.; Capelot, M.; Tournilhac, F.; Leibler, L. Silica-Like Malleable Materials from Permanent Organic Networks. Science **2011**, 334, 965-968; (b)Capelot, M.; Montarnal, D.; Tournilhac, F.; Leibler, L. Metal-Catalyzed Transesterification for Healing and Assembling of Thermosets. J. Am. Chem. Soc. **2012**, 134, 7664-7667; (c)Yang, S.; Chen, J.-S.; Körner, H.; Breiner, T.; Ober, C. K.; Poliks, M. D. Reworkable Epoxies: Thermosets with Thermally Cleavable Groups for Controlled Network Breakdown. Chem. Mater. **1998**, 10, 1475-1482.

(6) Wang, L.; Wong, C. P. Syntheses and characterizations of thermally reworkable epoxy resins. Part I. J. Polym. Sci., Part A: Polym. Chem. **1999**, 37, 2991-3001.

(7) Tesoro, G. C.; Sastri, V. Reversible crosslinking in epoxy resins. I. Feasibility studies. J. Appl. Polym. Sci. **1990**, 39, 1425-1437.

(8) Ying, H.; Zhang, Y.; Cheng, J. Dynamic urea bond for the design of reversible and self-healing polymers. Nat. Commun. **2014**, 5.

(9) (a)Reutenauer, P.; Buhler, E.; Boul, P. J.; Candau, S. J.; Lehn, J. M. Room Temperature Dynamic Polymers Based on Diels–Alder Chemistry. Chem. Eur. J. **2009**, 15, 1893-1900; (b)Chen, X.; Dam, M. A.; Ono, K.; Mal, A.; Shen, H.; Nutt, S. R.; Sheran, K.; Wudl, F. A Thermally Re-mendable Cross-Linked Polymeric Material. Science **2002**, 295, 1698-1702.

(10) Lu, Y.-X.; Tournilhac, F.; Leibler, L.; Guan, Z. Making Insoluble Polymer Networks Malleable via Olefin Metathesis. J. Am. Chem. Soc. **2012**, 134, 8424-8427.

(11) Denissen, W.; Winne, J. M.; Du Prez, F. E. Vitrimers: permanent organic networks with glass-like fluidity. Chem. Sci. **2016**, 7, 30-38.

(12) Yang, L.; Tan, X.; Wang, Z.; Zhang, X. Supramolecular Polymers: Historical Development, Preparation, Characterization, and Functions. Chem. Rev. **2015**, 115, 7196-7239.

(13) Wojtecki, R. J.; Meador, M. A.; Rowan, S. J. Using the dynamic bond to access macroscopically responsive structurally dynamic polymers. Nat. Mater. **2011**, 10, 14-27.

(14) Montero de Espinosa, L.; Fiore, G. L.; Weder, C.; Johan Foster, E.; Simon, Y. C. Healable supramolecular polymer solids. Prog. Polym. Sci. **2015**, 49–50, 60-78.

(15) Heinzmann, C.; Weder, C.; de Espinosa, L. M. Supramolecular polymer adhesives: advanced materials inspired by nature. Chem. Soc. Rev. **2015**.

(16) (a)Yamauchi, K.; Lizotte, J. R.; Hercules, D. M.; Vergne, M. J.; Long, T. E. Combinations of Microphase Separation and Terminal Multiple Hydrogen Bonding in Novel Macromolecules. J. Am. Chem. Soc. **2002**, 124, 8599-8604; (b)Yamauchi, K.; Kanomata, A.; Inoue, T.; Long, T. E. Thermoreversible Polyesters Consisting of Multiple Hydrogen Bonding (MHB). Macromolecules **2004**, 37, 3519-3522.

(17) Wojtecki, R. J.; Nelson, A. Small changes with big effects: Tuning polymer properties with supramolecular interactions. J. Polym. Sci., Part A: Polym. Chem. **2016**, 54, 457-472.

(18) Balkenende, D. W. R.; Monnier, C. A.; Fiore, G. L.; Weder, C. Optically responsive supramolecular polymer glasses. Nat. Commun. **2016**, 7.
(19) St.Pourcain, C. B.; Griffin, A. C. Thermoreversible Supramolecular Networks with Polymeric Properties. Macromolecules **1995**, 28, 4116-4121.
(20) (a)Kato, T.; Fréchet, J. M. J. Stabilization of a liquid-crystalline phase through noncovalent interaction with a polymer side chain. Macromolecules **1989**, 22, 3818-3819; (b)Kato, T.; Kihara, H.; Uryu, T.; Fujishima, A.; Fréchet, J. M. J. Molecular self-assembly of liquid crystalline side-chain polymers through intermolecular hydrogen bonding. Polymeric complexes built from a polyacrylate and stilbazoles. Macromolecules **1992**, 25, 6836-6841; (c)Kato, T.; Kihara, H.; Kumar, U.; Uryu, T.; Fréchet, J. M. J. A Liquid-Crystalline Polymer Network Built by Molecular Self-Assembly through Intermolecular Hydrogen Bonding. Angew. Chem. Int. Ed. **1994**, 33, 1644-1645; (d)Kihara, H.; Kato, T.; Uryu, T.; Fréchet, J. M. J. Supramolecular Liquid-Crystalline Networks Built by Self-Assembly of Multifunctional Hydrogen-Bonding Molecules. Chem. Mater. **1996**, 8, 961-968; (e)Kato, T.; Mizoshita, N.; Kishimoto, K. Functional Liquid-Crystalline Assemblies: Self-Organized Soft Materials. Angew. Chem. Int. Ed. **2006**, 45, 38-68.
(21) (a)Wiegel, K. N.; Griffin, A. C.; Black, M. S.; Schiraldi, D. A. Memory effects in supramolecular networks of diacids and polyfunctional pyridine derivatives. J. Appl. Polym. Sci. **2004**, 92, 3097-3106; (b)Greuel, J. R.; Andrews, T. E.; Wichman, J. J.; Tessner, J. D.; Wiegel, K. N. Supramolecular main-chain liquid crystalline polymers and networks with competitive hydrogen bonding: networks and linear polymers created from tris- and bis-functionalised pyridyl networking agents. Liq. Cryst. **2010**, 37, 1515-1520; (c)Miesen, R. F.; Friday, S. R.; Wiegel, K. N. Supramolecular main-chain liquid crystalline polymers and networks with competitive hydrogen bonding: a study of flexible bis-acids and a mixture of rigid and flexible polypyridyls. Liq. Cryst. **2011**, 38, 1341-1347.
(22) Lin, H.-C.; Hendrianto, J. Synthesis and characterization of H-bonded side-chain and crosslinking LC polymers containing donor/acceptor homopolymers and copolymers. Polymer **2005**, 46, 12146-12157.
(23) Shan, N.; Bond, A. D.; Jones, W. Crystal engineering using 4,4′-bipyridyl with di- and tricarboxylic acids. Cryst. Eng. **2002**, 5, 9-24.
(24) Kato, T.; Adachi, H.; Fujishima, A.; Fréchet, J. M. J. Self-Assembly of Liquid Crystalline Complexes Having Angular Structures through Intermolecular Hydrogen Bonding. Chem. Lett. **1992**, 21, 265-268.
(25) Montero de Espinosa, L.; Balog, S.; Weder, C. Isophthalic Acid–Pyridine H-Bonding: Simplicity in the Design of Mechanically Robust Phase-Segregated Supramolecular Polymers. ACS Macro Lett. **2014**, 3, 540-543.
(26) Cordier, P.; Tournilhac, F.; Soulie-Ziakovic, C.; Leibler, L. Self-healing and thermoreversible rubber from supramolecular assembly. Nature **2008**, 451, 977-980.
(27) De Goffau, M. C.; Yang, X.; Van Dijl, J. M.; Harmsen, H. J. M. Bacterial pleomorphism and competition in a relative humidity gradient. Environ. Microbiol. **2009**, 11, 809-822.
(28) Down, J. L. The Yellowing of Epoxy Resin Adhesives: Report on Natural Dark Aging. Studies in Conservation **1984**, 29, 63-76.
(29) Kato, T.; Fréchet, J. M. J. A new approach to mesophase stabilization through hydrogen bonding molecular interactions in binary mixtures. J. Am. Chem. Soc. **1989**, 111, 8533-8534.

(30) (a)Shirota, Y. Organic materials for electronic and optoelectronic devices. Journal of Materials Chemistry **2000**, 10, 1-25; (b)Ishikawa, W.; Noguchi, K.; Kuwabaru, Y.; Shirota, Y. Novel amorphous molecular materials: The starburst molecule 1,3,5-tris[N-(4-diphenyl- aminophenyl)phenylamino]benzene. Advanced Materials **1993**, 5, 559-561; (c)Katsuma, K.; Shirota, Y. A Novel Class of π-Electron Dendrimers for Thermally and Morphologically Stable Amorphous Molecular Materials. Advanced Materials **1998**, 10, 223-226.

(31) Burattini, S.; Greenland, B. W.; Merino, D. H.; Weng, W.; Seppala, J.; Colquhoun, H. M.; Hayes, W.; Mackay, M. E.; Hamley, I. W.; Rowan, S. J. A Healable Supramolecular Polymer Blend Based on Aromatic π–π Stacking and Hydrogen-Bonding Interactions. J. Am. Chem. Soc. **2010**, 132, 12051-12058.

(32) Agnaou, R.; Capelot, M.; Tencé-Girault, S.; Tournilhac, F.; Leibler, L. Supramolecular Thermoplastic with 0.5 Pa·s Melt Viscosity. J. Am. Chem. Soc. **2014**, 136, 11268-11271.

(33) (a)Shabbir, A.; Goldansaz, H.; Hassager, O.; van Ruymbeke, E.; Alvarez, N. J. Effect of Hydrogen Bonding on Linear and Nonlinear Rheology of Entangled Polymer Melts. Macromolecules **2015**, 48, 5988-5996; (b)Callies, X.; Véchambre, C.; Fonteneau, C.; Pensec, S.; Chenal, J. M.; Chazeau, L.; Bouteiller, L.; Ducouret, G.; Creton, C. Linear Rheology of Supramolecular Polymers Center-Functionalized with Strong Stickers. Macromolecules **2015**, 48, 7320-7326.

(34) Heinzmann, C.; Coulibaly, S.; Roulin, A.; Fiore, G. L.; Weder, C. Light-induced bonding and debonding with supramolecular adhesives. ACS Appl. Mater. Interfaces **2014**, 6, 4713-9.

(35) Fiore, G. L.; Rowan, S. J.; Weder, C. Optically healable polymers. Chem. Soc. Rev. **2013**, 42, 7278-7288.

(36) Heinzmann, C.; Salz, U.; Moszner, N.; Fiore, G. L.; Weder, C. Supramolecular Cross-Links in Poly(alkyl methacrylate) Copolymers and Their Impact on the Mechanical and Reversible Adhesive Properties. ACS Appl. Mater. Interfaces **2015**, 7, 13395-13404.

TOC Entry

Epoxy resin-inspired reconfigurable supramolecular networks

Diederik W. R. Balkenende, Rebecca Anne Olson, Sandor Balog, Christoph Weder and Lucas Montero de Espinosa